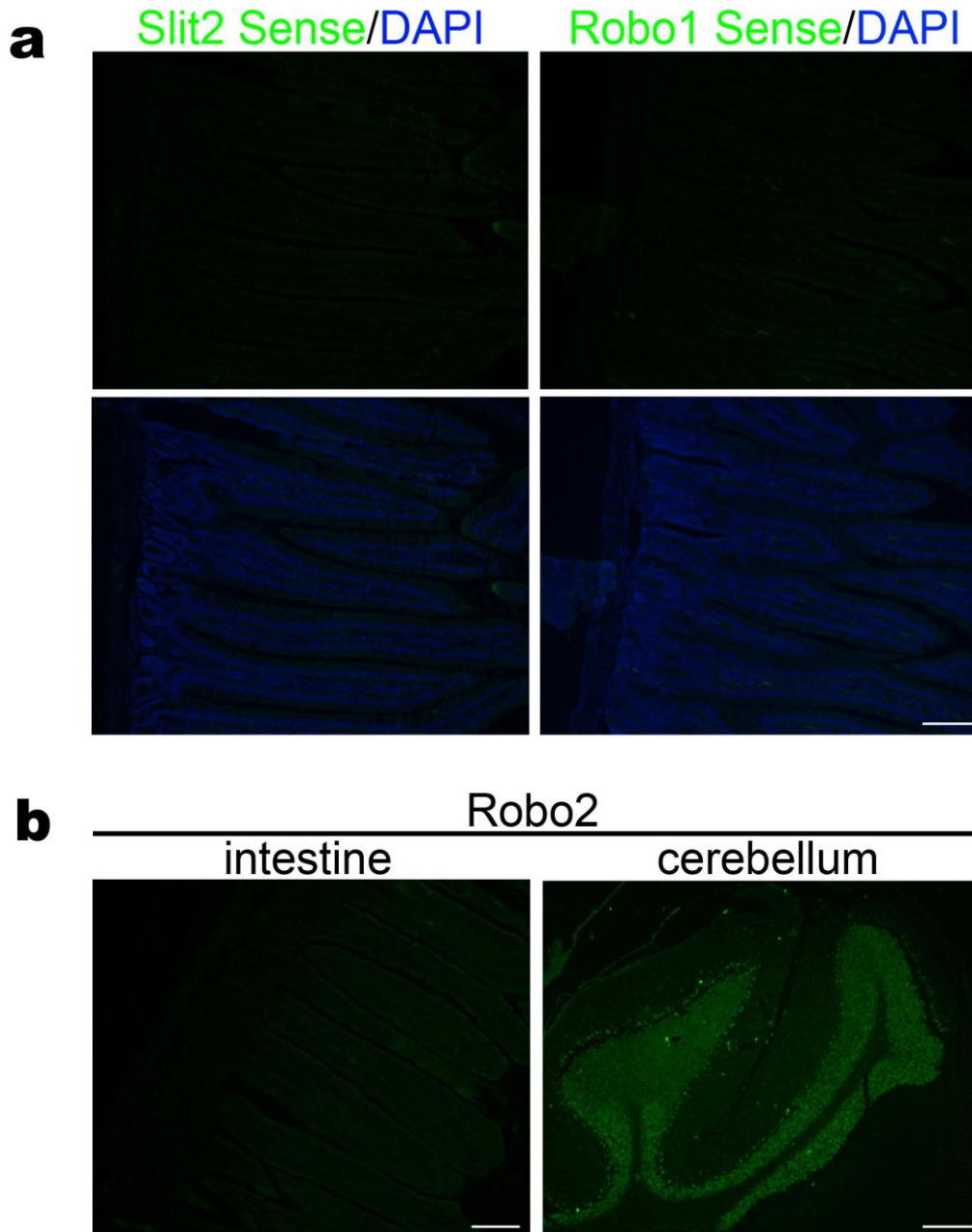


Induction of intestinal stem cells by R-spondin 1 and Slit2 augments chemoradioprotection

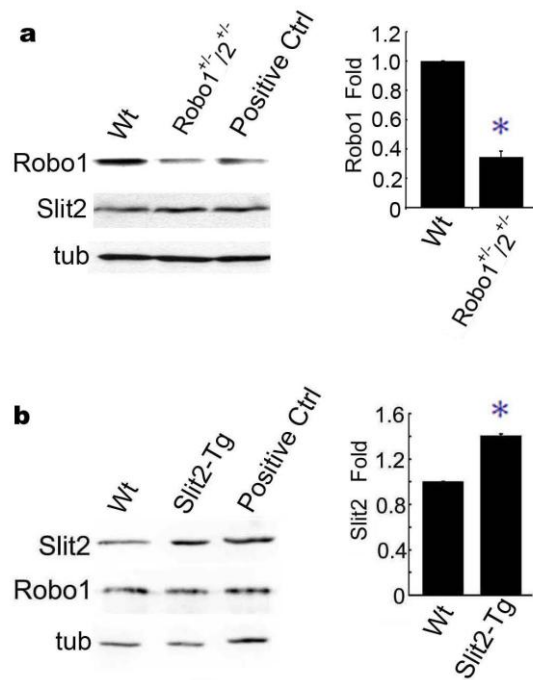
Wei-Jie Zhou, Zhen H. Geng, Jason R. Spence, and Jian-Guo Geng

SUPPLEMENTARY FIGURE LEGENDS



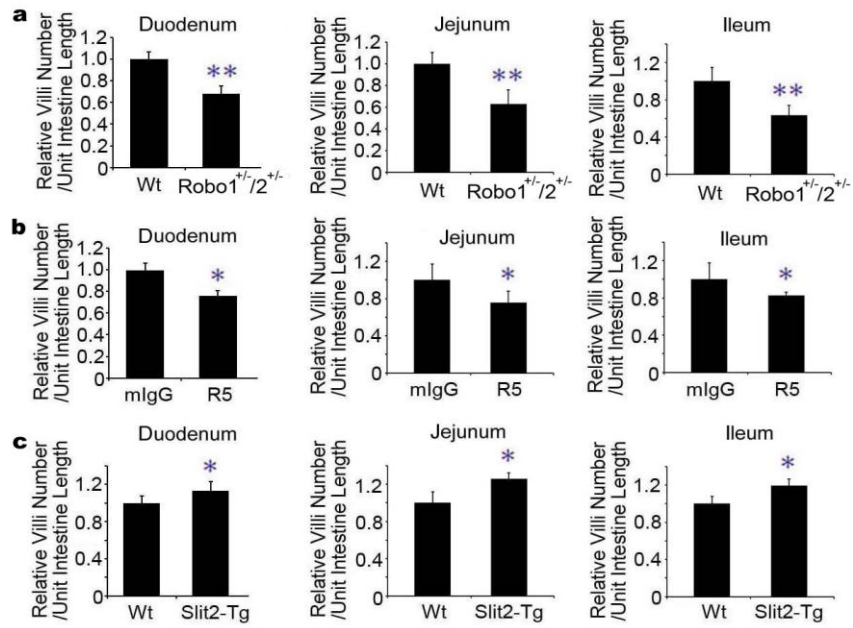
Supplementary Figure 1 RNA probe specificity and Robo2 mRNA expression. Tissue specimens of the small intestine and the cerebellum obtained from Wt mice (8 weeks old) were stained by using the sense Robo1 and Slit2 RNA probes (**a**) or the antisense Robo2 RNA probe (**b**). Sections were counterstained with DAPI (**a**, lower panel). Results are representatives of more than three separate experiments. Bar, 50 μ M for **a**, **b** (small intestine);

200 μm for **b** (cerebellum).

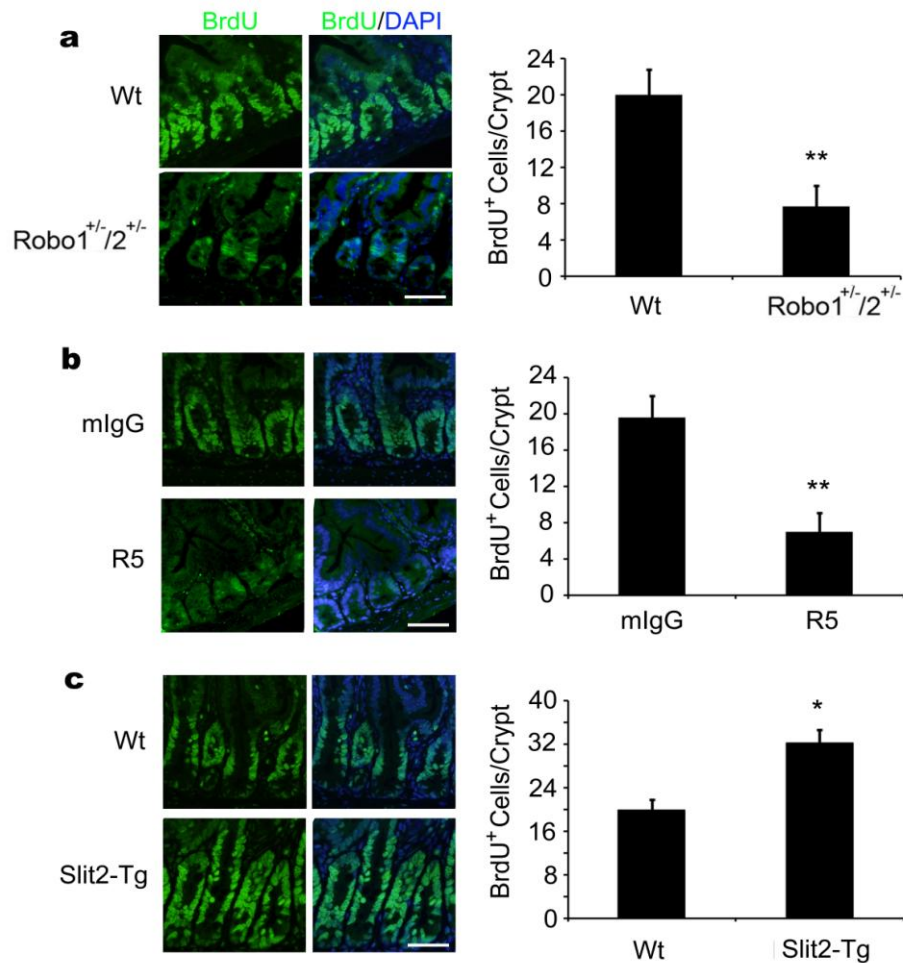


Supplementary Figure 2 Characterization of *Robo1*^{+/2+/-}; *Robo2*^{+/2+/-} and *Slit2*-Tg mice.

Lysates of the small intestinal crypts isolated from Wt, *Robo1*^{+/2+/-} and *Slit2*-Tg mice (8 weeks old) were immunoblotted by affinity purified rabbit anti-Slit2 or rabbit anti-Robo1 polyclonal Abs and the α -tubulin Ab (tub; **a**, **b**, left panels). The lysate of human colorectal epithelial HCT116 cells stably expressing Slit2 and Robo1 was also immunoblotted as a positive control (Positive Ctrl) for Robo1 (**a**), and the supernatant from 293 cells stably expressing human Slit2 was used as positive control for Slit2 (**b**). The immunoblotting densities for Robo1 (**a**, right panel) and Slit2 (**b**, right panel) are shown. Results represent at least three separate experiments. *, $p < 0.05$.



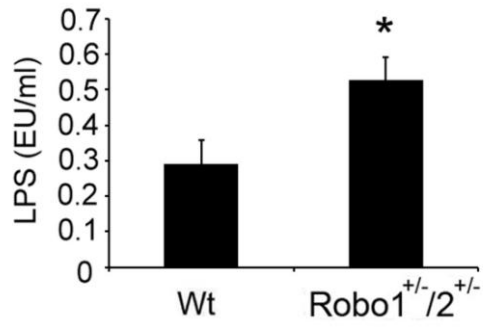
Supplementary Figure 3 Distorted villi in small intestine. The numbers of villi per unit length of duodenum, jejunum and ileum (a-c) were counted double-blindly in Wt littermates and *Robo1/2* mutants, Wt mice treated with mIgG and R5, or Wt and *Slit2-Tg* mice. Results represent fifty tissue specimens in each group (five mice/group; 8 weeks old) and the mean \pm S.D. of 10 tissue sections/mouse. *, $p < 0.05$; **, $p < 0.01$.



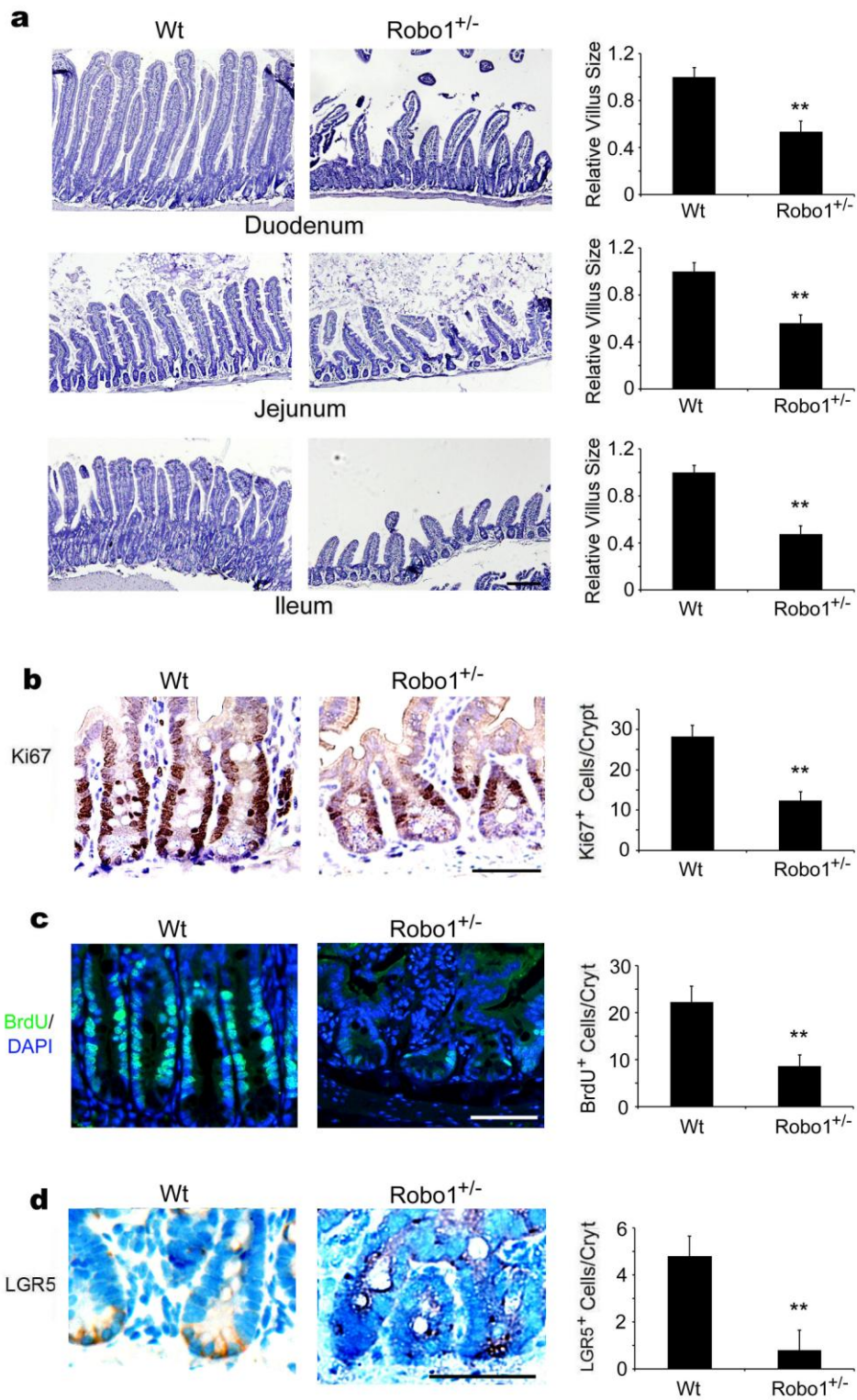
Supplementary Figure 4 Effects of Slit-Robo signaling on intestinal cell proliferation.

BrdU was injected into Wt littermates and *Robo1/2* mutants (a), Wt mice treated with mIgG and R5 (b), or Wt and *Slit2-Tg* mice (c). The harvested tissue specimens of the small intestines were stained for BrdU (green) and cell nuclei (DAPI; blue). The positive proliferating intestinal cells were then quantified. Results represent fifty tissue specimens in each group (five mice/group; 8 weeks old) and the mean \pm S.D. of 10 tissue sections/mouse.

*, $p < 0.05$; **, $p < 0.01$. Bars, 50 μ m.

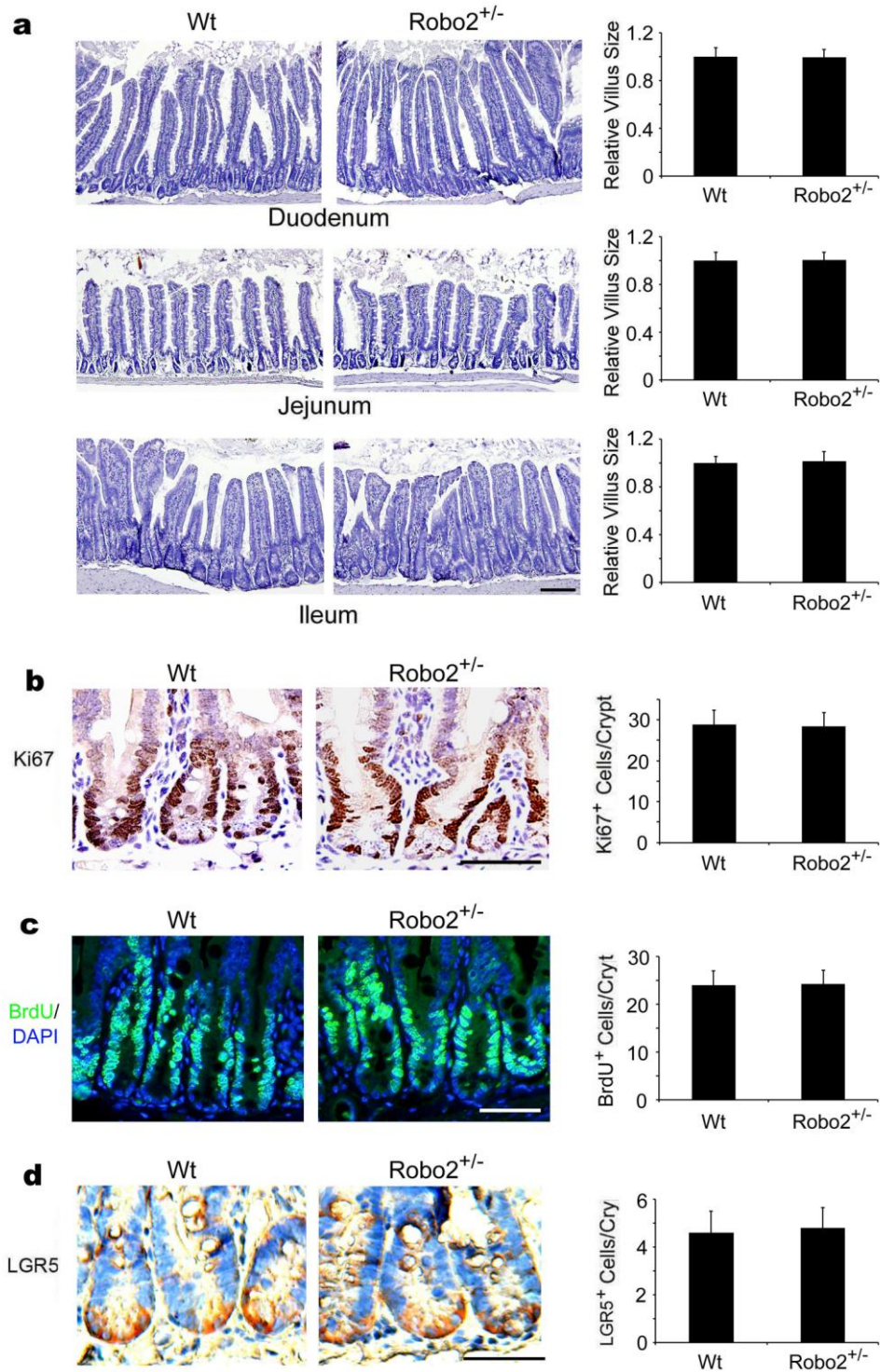


Supplementary Figure 5 Determination of serum endotoxin. Blood samples were obtained from Wt littermates and *Robo1*^{+/-}/*2*^{+/-} mice and serum levels of lipopolysaccharides (LPS) were measured according to the Lonza's protocol. Results are the mean \pm S.D. (five mice/group; 8 weeks old). *, $p < 0.05$.



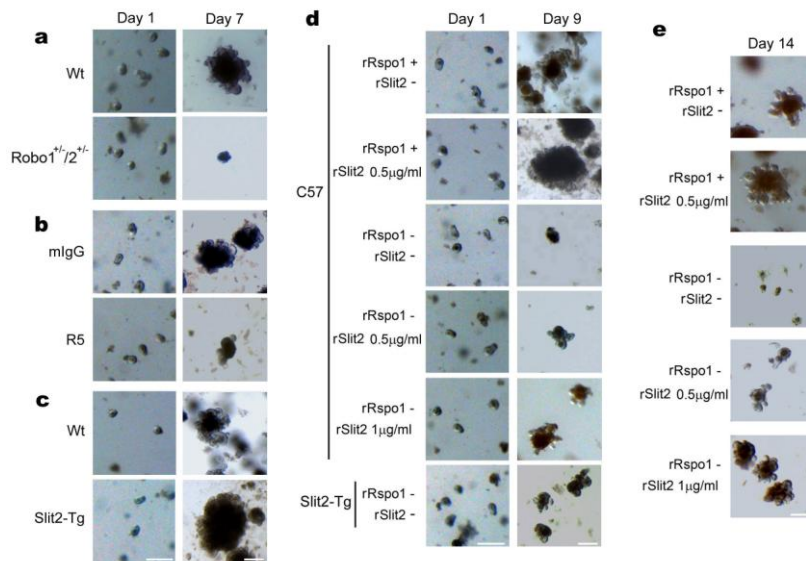
Supplementary Figure 6 Phenotypic aberrations in the *Robo1*^{+/-} small intestine. a, Microscopic morphology of mouse small intestines. Sections of paraffin-embedded small intestines from Wt littermates and *Robo1*^{+/-} mice (8 weeks old) were H&E stained. Relative

villus sizes were measured and statistically analyzed. **b-d**, Effects of partial *Robo1* deficiency on the number and distribution of intestinal cells. Tissue sections of small intestines from Wt littermates and *Robo1*^{+/-} mice were immunohistochemically stained for Ki67⁺-TA cells (**b**), BrdU⁺-intestinal cells (**c**) and LGR5⁺-ISCs (**d**). The numbers of positive cells were counted in each crypt. Results represent fifty tissue specimens in each group (five mice/group; 8 weeks old) and the mean \pm S.D. measurements of 10 tissue sections/mouse. Bars, 200 μ m for **a**, and 50 μ m for **b-d**. **, $p < 0.01$.

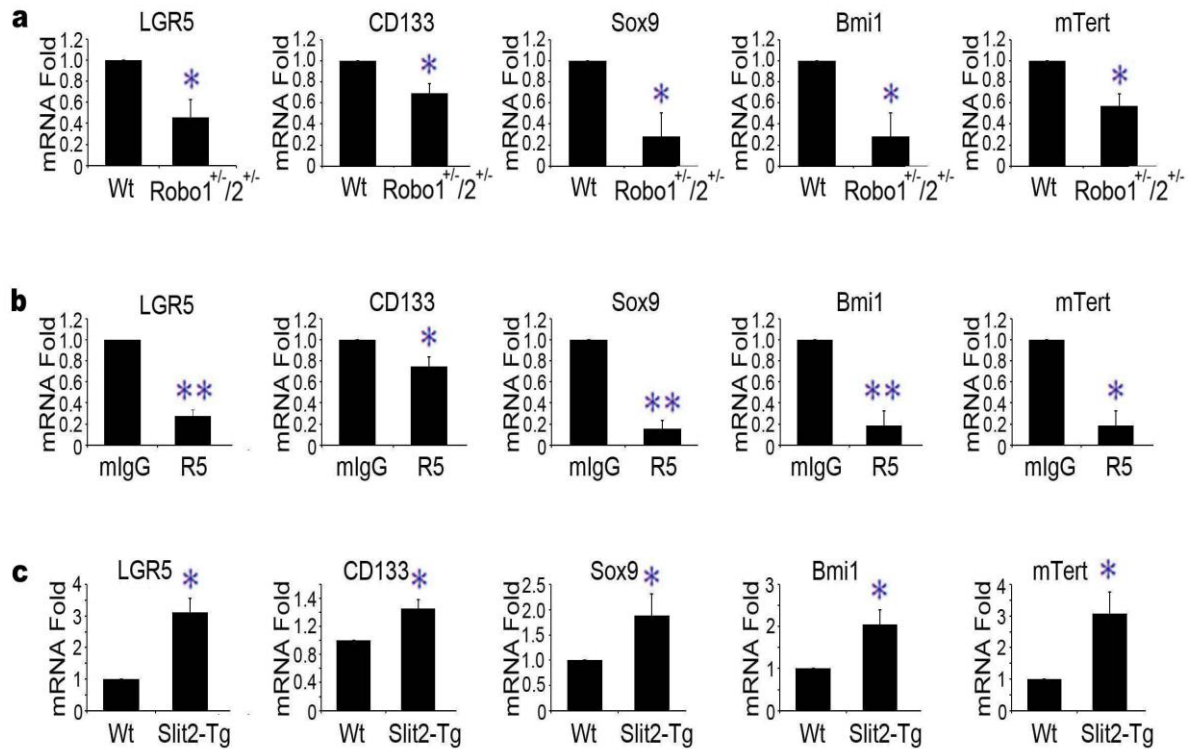


Supplementary Figure 7 Phenotypic aberrations in the *Robo2*^{+/-} small intestine. a, Microscopic morphology of mouse small intestines. Sections of paraffin-embedded small intestines from Wt littermates and *Robo2*^{+/-} mice (8 weeks old) were H&E stained. Relative villus sizes were measured and statistically analyzed. **b-d,** Effects of partial *Robo2* deficiency

on the number and distribution of intestinal cells. Tissue sections of small intestines from Wt littermates and *Robo2*^{+/-} mice were immunohistochemically stained for Ki67⁺-TA cells (**b**), BrdU⁺-intestinal cells (**c**) and LGR5⁺-ISCs (**c**). The numbers of positive cells were counted in each crypt. Results represent fifty tissue specimens in each group (five mice/group; 8 weeks old) and the mean \pm S.D. of 10 tissue sections/mouse. Bars, 100 μ m for **a** and 50 μ m for **b-d**.

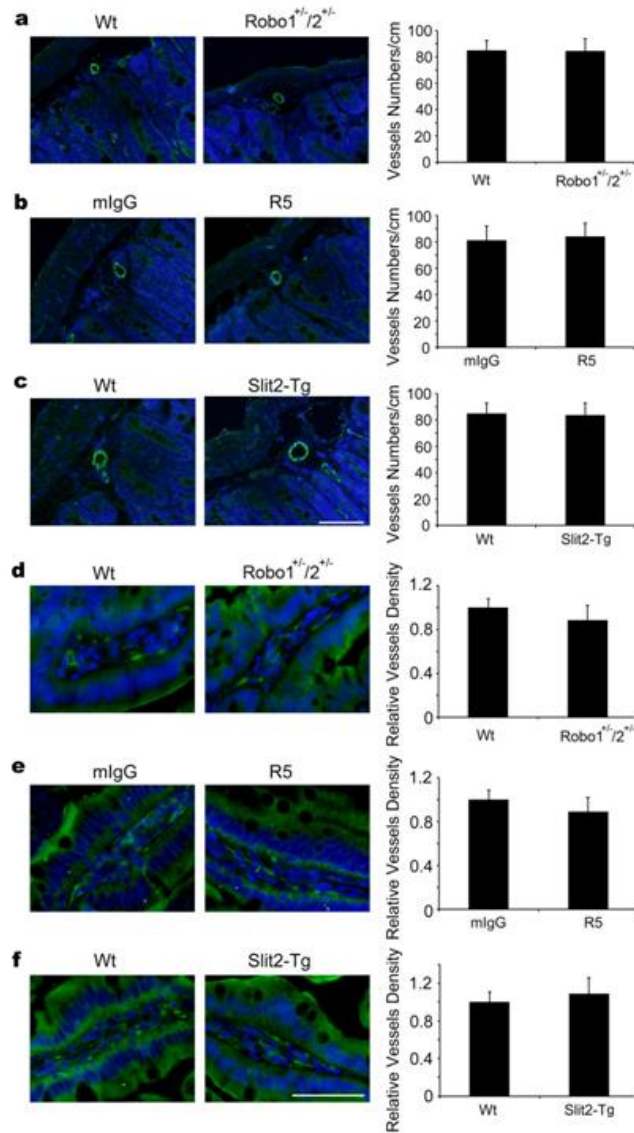


Supplementary Figure 8 Enlarged images for cultured intestinal organoids. The intestinal crypts were isolated from Wt littermates and *Robo1*^{+/-}/*2*^{+/-} mice (a), mIgG and R5-treated Wt mice (b), and Wt and *Slit2*-Tg mice (c). They were *in vitro* cultured into intestinal organoids according to the published methods⁵⁻⁸. In addition, the Wt intestinal crypts were cultured in the presence of rRspo1 (without rSlit2) or rRspo1 plus rSlit2, in the absence of both rRspo1 and rSlit2, and in the presence of rSlit2 (without rRspo1) (d; top five panels). The intestinal crypts were also isolated from *Slit2*-Tg mice and *in vitro* cultured in the absence of both rRspo1 and rSlit2 (d; bottom panel). Also, the intestinal crypts were isolated from LGR5-GFP mice¹⁵. After cell sorting for GFP⁵, GFP^{high}-ISCs were cultured in the presence of rRspo1 (without rSlit2) or rRspo1 plus rSlit2, in the absence of both rRspo1 and rSlit2, and in the presence of rSlit2 (without rRspo1) (e). All mice used were 8 weeks old. Results represent at least the triplicates of three separate experiments. Bars, 200 µm.

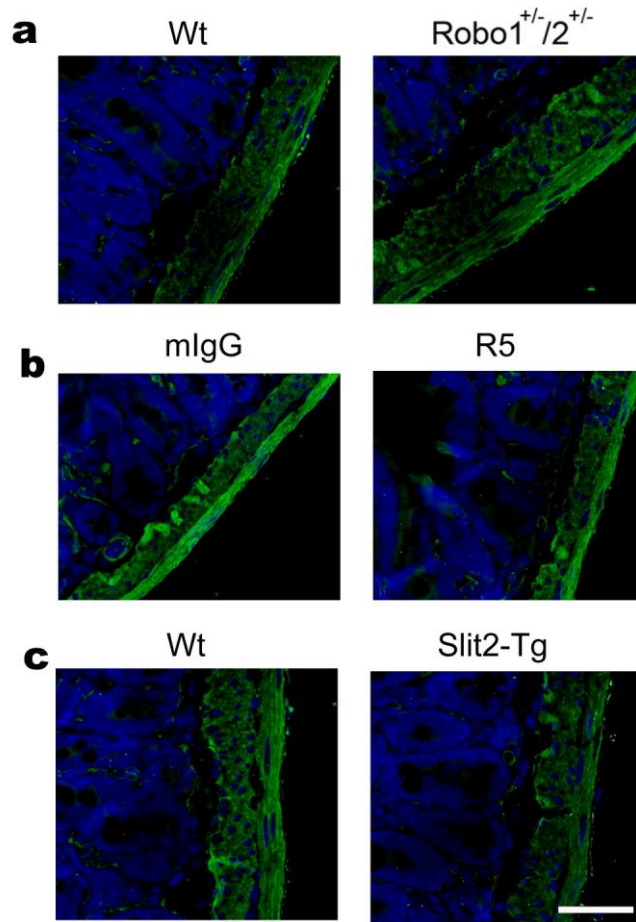


Supplementary Figure 9 Intestinal expression of LGR5, CD133, Sox9, Bmi1 and mTert.

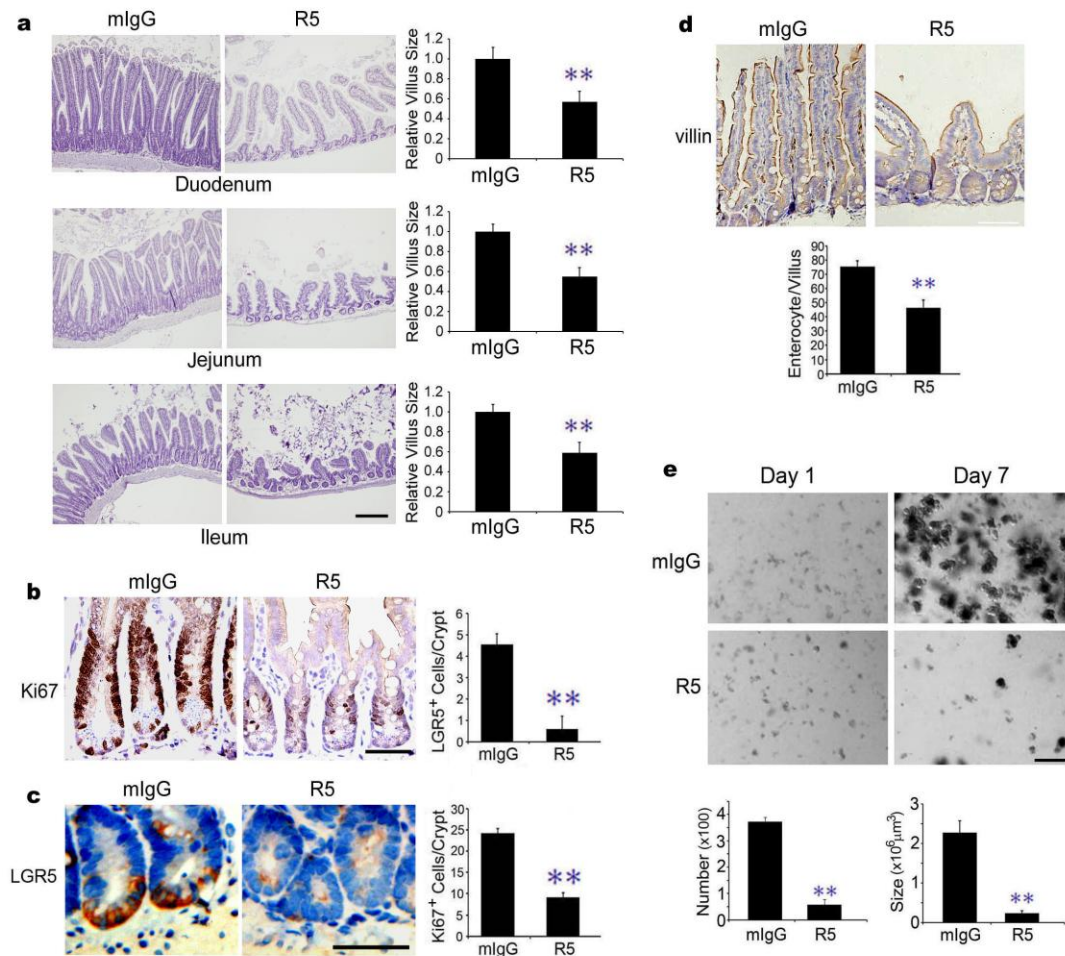
Total RNA was extracted from the small intestinal crypts of Wt littermates and *Robo1*^{+/-}/*2*^{+/-} mice (a), mIgG and R5-treated Wt mice (b), and Wt and *Slit2*-Tg mice (c). These were reverse transcribed, PCR amplified and normalized to an endogenous β -actin control. Results represent the mean \pm S.D. (5 mice/group; 8 weeks old). *, $p < 0.05$; **, $p < 0.01$.



Supplementary Figure 10 Localization of vascular endothelial cells in the small intestines. The tissue specimens of small intestines were harvested from Wt littermates and *Robo1/2* mutants (**a, d**), mIgG and R5-treated Wt mice (**b, e**) and Wt and *Slit2*-Tg mice (**c, f**). They were stained for endothelial cells (CD31; green) and cell nuclei (DAPI; blue) and statistically analyzed. Results are representative images and the mean \pm S.D. of 10 tissue sections/mouse (five mice/group; 8 weeks old). Bar, 50 μ m.

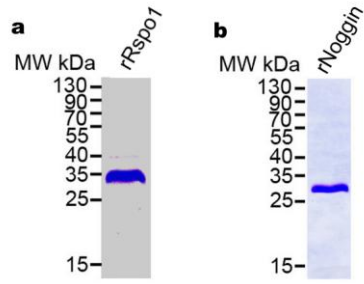


Supplementary Figure 11 Distribution of smooth muscle cells in the small intestines. The tissue specimens of small intestines were harvested from Wt littermates and *Robo1/2* mutants (top panel), mIgG and R5-treated Wt mice (middle panel) and Wt and *Slit2*-Tg mice (bottom panel). They were stained for smooth muscle cells (α -smooth muscle actin; green) and cell nuclei (DAPI; blue). Results are representative images of 10 tissue sections/mouse (five mice/group; 8 weeks old). Bar, 50 μ m.

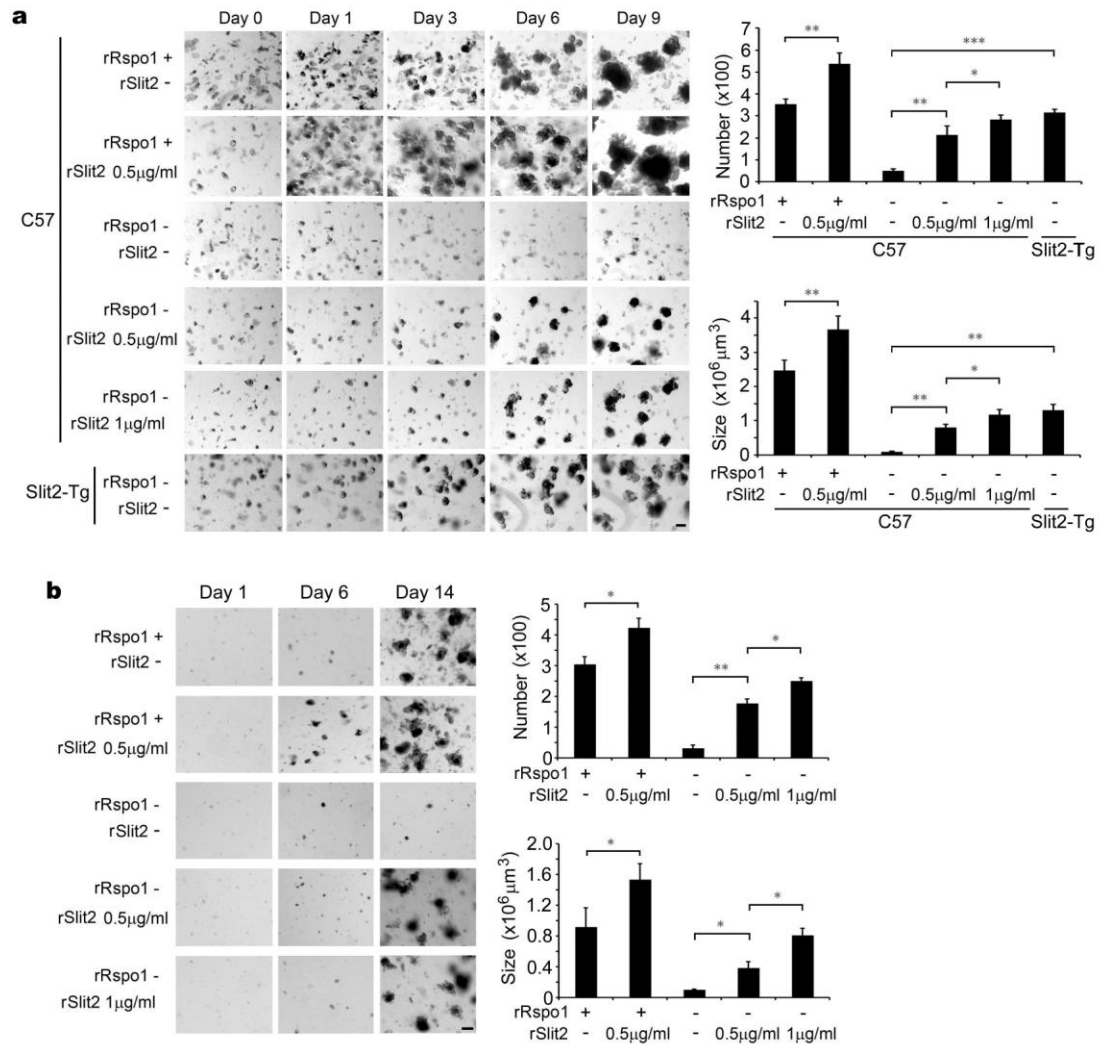


Supplementary Figure 12 Neutralization of Slit2 binding to Robo1 retards small intestinal regeneration. **a**, Effects of R5 on intestinal histology. Wt mice (8 weeks old) were treated daily with mIgG or R5 for 6 consecutive days. Small intestines were stained with H&E, and the relative villus sizes were measured and statistically analyzed. **b-d**, Impact of R5 on the number and distribution of intestinal cells. Wt mice were treated with mIgG or R5, and their small intestines were immunohistochemically stained for Ki67 (**b**), LGR5 (**c**) and villin (**d**). The numbers of positive cells were counted in each crypt. **e**, Effects of R5 on the formation of intestinal organoids. The intestinal crypts isolated from Wt mice were *in vitro* cultured⁴⁻⁷ in the presence of mIgG or R5. The numbers and sizes were measured on day 7. Results represent fifty tissue specimens in each group (five mice/group; 8 weeks old) and the

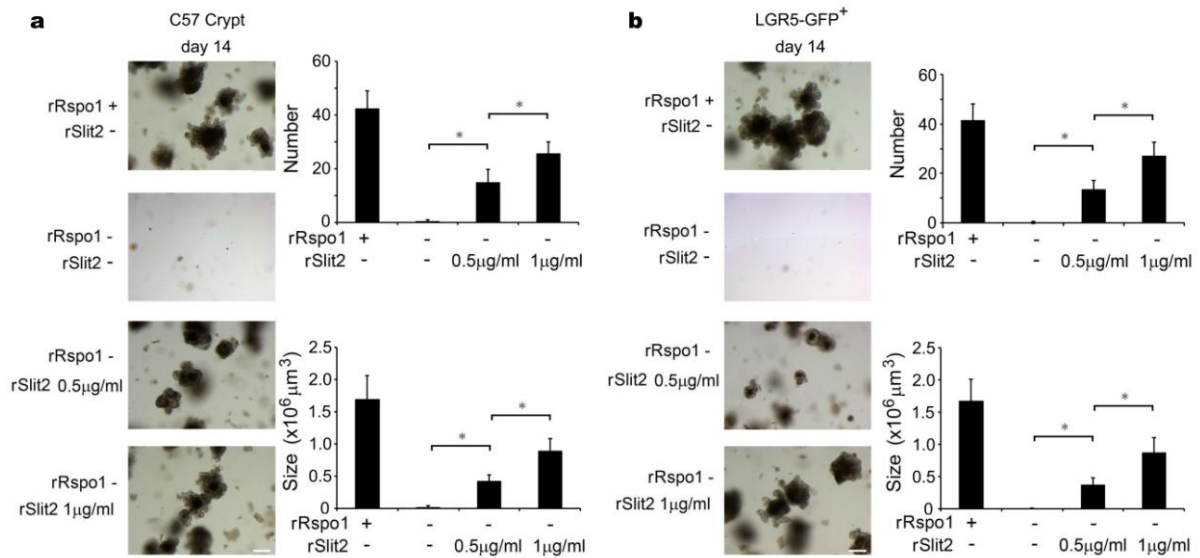
mean \pm S.D. of 10 tissue sections/mouse. Bars, 100 μm for **a**, **e** and 50 μm for **b-d**. **, $p < 0.01$.



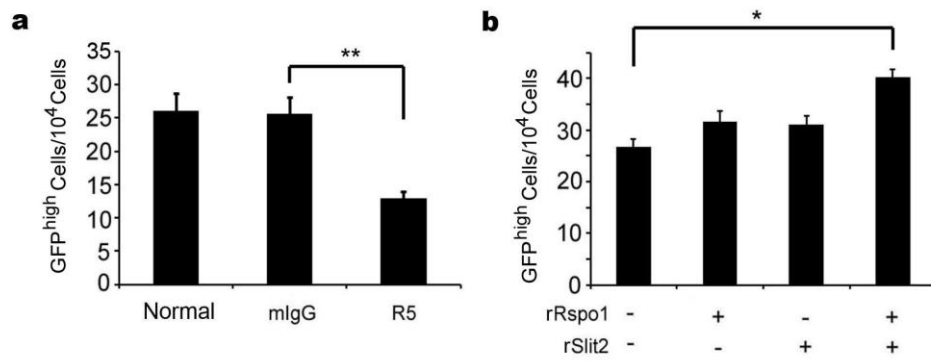
Supplementary Figure 13 Purification of rRspo1 and rNoggin. Coomassie blue staining of purified rRspo1 (**a**) and rNoggin (**b**) under reducing conditions. Results are representatives of three or more separate protein preparations.



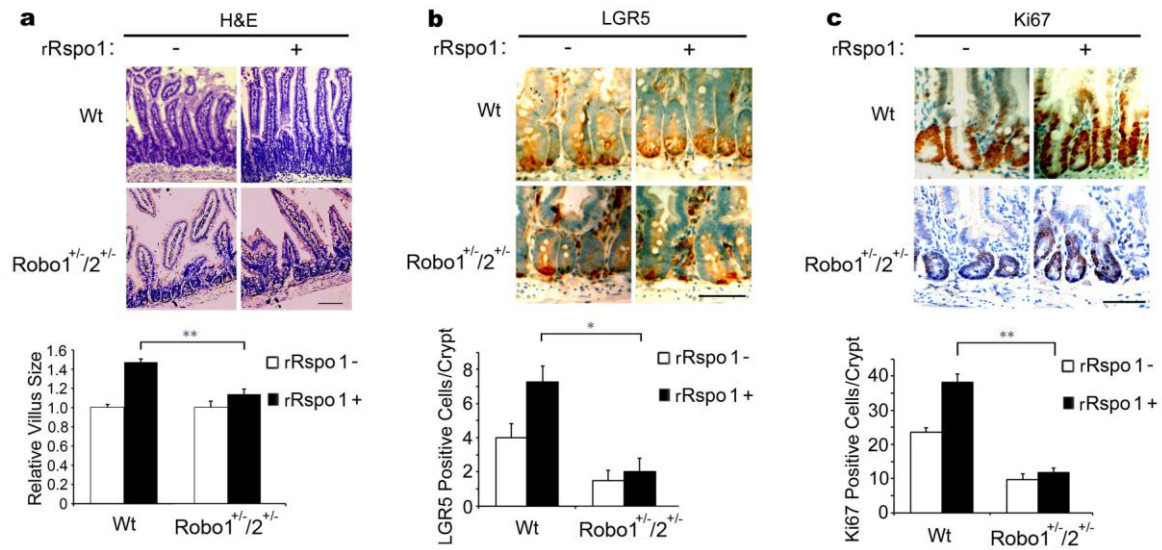
Supplementary Figure 14 Slit2 substitutes and potentiates Rspo1 for induction of intestinal organoids. The intestinal crypts (a) and LGR5⁺-ISCs (b) were isolated from Wt, *Slit2*-Tg and LGR5-GFP mice and cultured *in vitro* in the presence of rRspo1, rRspo1 plus rSlit2, in the absence of rRspo1, in the absence of rRspo1 but in the presence of rSlit2, or in the absence of both rRspo1 and rSlit2. The numbers and sizes of intestinal organoids were measured. Results represent at least the triplicates of three separate experiments. Bars, 200 μm . *, $p < 0.05$; **, $p < 0.01$; ***, $p < 0.001$.



Supplementary Figure 15 Effects of Slit2 and Rspo1 for serial passage of intestinal organoids. The intestinal crypts (a) and LGR5⁺-ISCs (b) were isolated from Wt mice and LGR5-GFP mice (8 weeks old) and cultured *in vitro* in the presence of rRspo1 (without rSlit2), in the absence of both rRspo1 and rSlit2, and in the presence of rSlit2 (without rRspo1). The intestinal organoids were separated into single crypts and passaged every 14 days up to the 4th passage⁴⁻⁷. Results represent three separate experiments on day 14 of fourth passage and the mean \pm S.D. in triplicates. Bars, 100 μm .



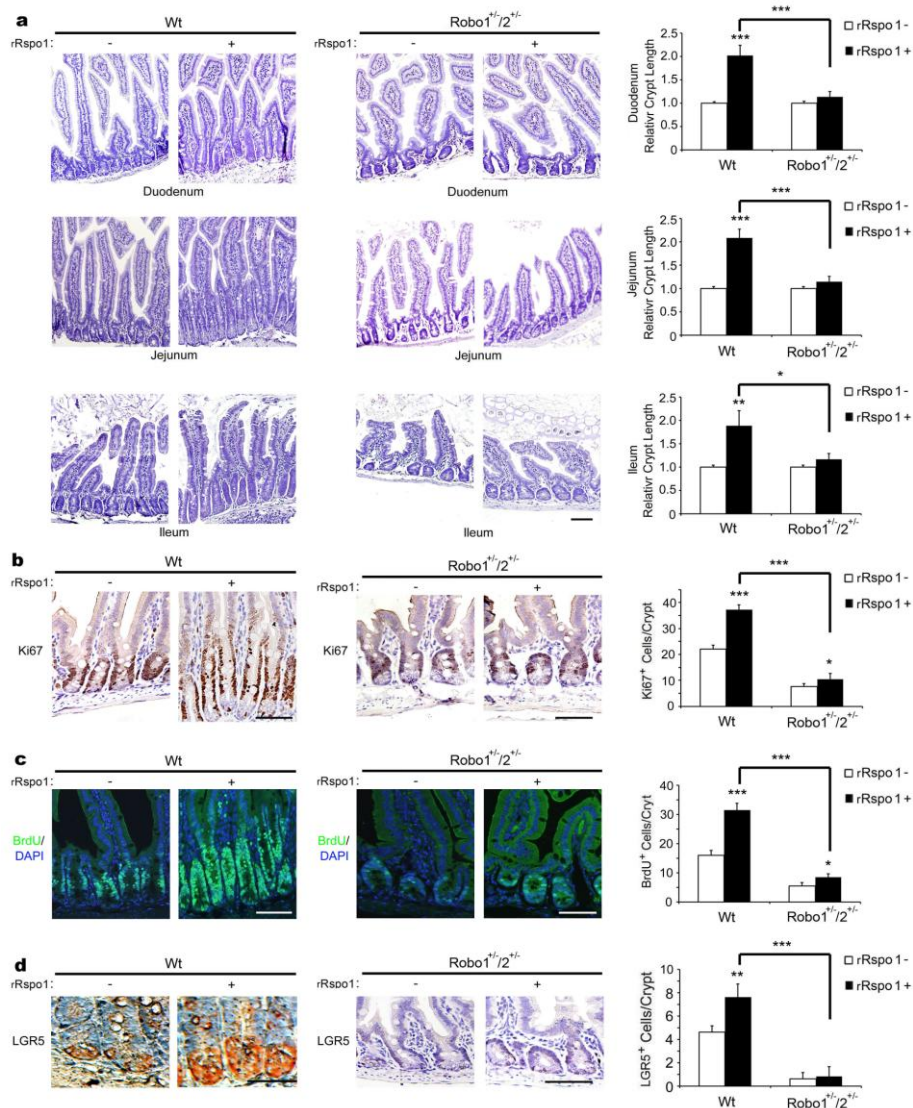
Supplementary Figure 16 *In vivo* effects of Slit-Robo signaling on GFP^{high}-intestinal crypt cells. **a**, R5 inhibits GFP^{high}-intestinal crypt cells. LGR5-GFP mice (8 weeks old) were given mIgG or R5 daily for 6 days and the crypt specimens of their small intestines were harvested on day 7. Following staining with the anti-GFP Ab, they were quantified by flow cytometry. **b**, Slit2 cooperates with Rspo1 for induction of GFP^{high}-intestinal crypt cells. LGR5-GFP mice (8 weeks old) were given saline (-), rRspo1, rSlit2 or rRspo1 plus rSlit2 daily for 3 days and the crypt specimens of their small intestines were harvested on day 6. Following staining with the anti-GFP Ab, they were quantified by flow cytometry. Results are the mean \pm S.D. of cytometric analysis for each group (five mice/group; 8 weeks old). *, $p < 0.05$; **, $p < 0.01$.



Supplementary Figure 17 Rspo1 fails to rescue the intestinal phenotypes in *Robo1/2*

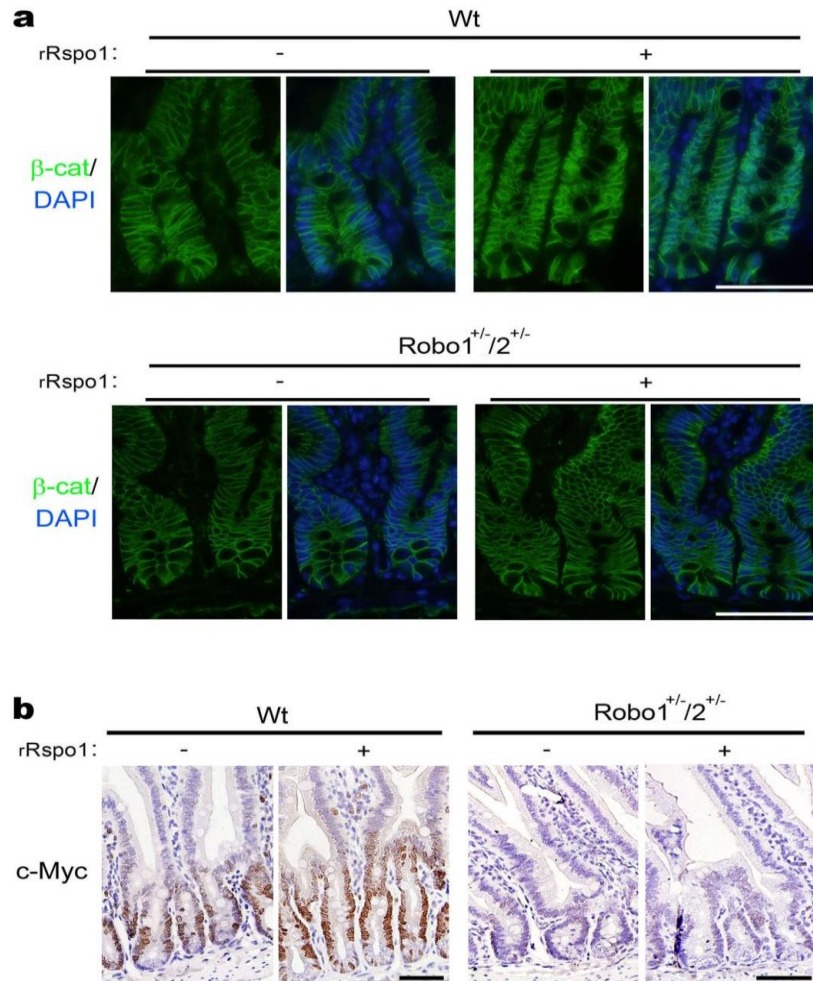
mutants. rRspo1 (0.1 mg/mouse/day for 5 days) was injected through the tail veins to Wt and *Robo1*^{+/2+/-}; *Robo2*^{+/2+/-} mice daily for 5 consecutive days. Mice were sacrificed at day 6 and the jejunum tissues harvested were H&E stained for determination of the relative villus sizes (a) and immunohistochemically stained for measurement of the numbers of LGR5⁺-ISCs (b) and Ki67⁺-TA cells (c). Results are the mean ± S.D. of 10 tissue sections/mouse (5 mice/group).

Bars, 50 μm. *, $p < 0.05$; **, $p < 0.01$.

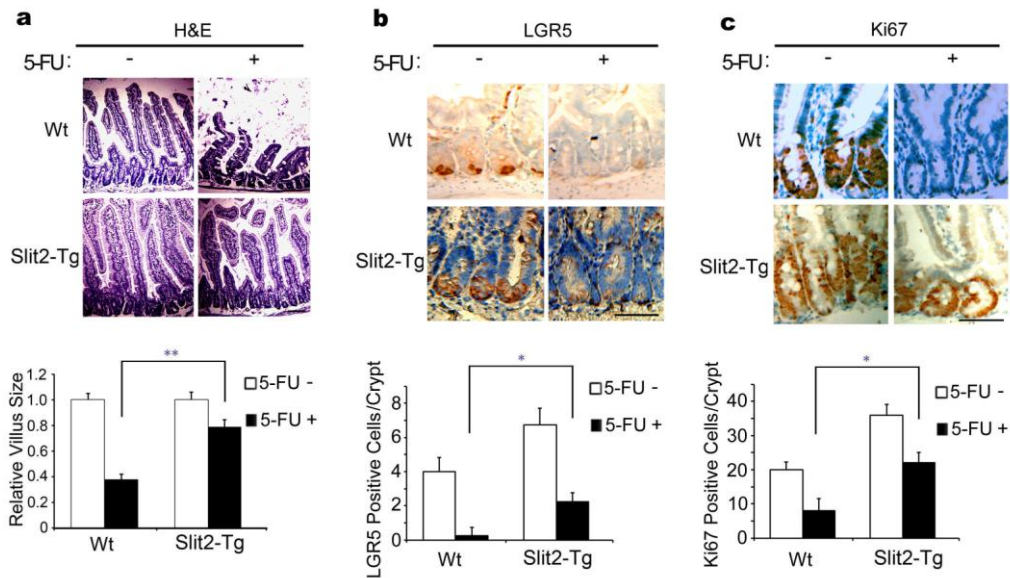


Supplementary Figure 18 Effects of a prolonged pulse of Rspo1 on intestinal regeneration in *Robo1/2* mutants. **a**, Effects of Rspo1 on intestinal morphology. Wt littermates and *Robo1/2* mutants (8 weeks old) were given rRspo1 (0.1 mg/mouse daily for 10 days) and the small intestines were harvested on day 11. The tissue specimens were stained with H&E, and the relative crypt sizes were measured and statistically analyzed. **b-d**, Effects of Rspo1 on the number and distribution of intestinal cells. The small intestines obtained from rRspo1-treated Wt littermates and *Robo1/2* mutant mice were immunohistochemically stained for Ki67⁺-TA cells (**b**), BrdU⁺-intestinal cells (**c**), and

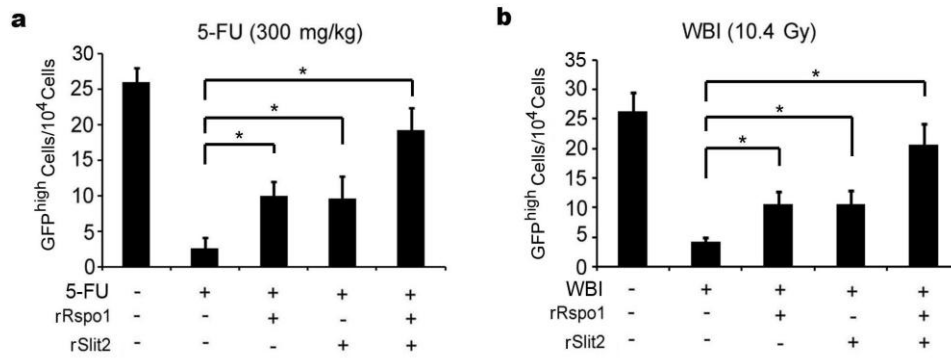
LGR5⁺-ISCs (**d**). The numbers of positive cells were counted in each crypt. Results represent fifty tissue specimens in each group (five mice/group; 8 weeks old) and the mean \pm S.D. of 10 tissue sections/mouse. Bars, 50 μ m for **a-d**. *, $p < 0.05$; ***, $p < 0.001$.



Supplementary Figure 19 Effects of a prolonged pulse of Rspo1 on canonical Wnt signaling in *Robo1/2* mutants. **a**, Rspo1 induces β -catenin translocation. Wt littermates and *Robo1/2* mutants were given rRspo1 (0.1 mg/mouse daily for 10 days) and the small intestines were harvested on day 11. The tissue specimens were stained for β -catenin (green) and cell nuclei (DAPI; blue). **b**, Rspo1 elevates expression of canonical Wnt targeting genes. The small intestines obtained from rRspo1-treated Wt littermates and *Robo1/2* mutant mice were immunohistochemically stained for c-Myc. Results represent fifty tissue specimens in each group (five mice/group; 8 weeks old). Bars, 50 μ m.



Supplementary Figure 20 *Slit2-Tg* intestines are less vulnerable to chemotherapy. Wt and *Slit2-Tg* mice were treated daily by intraperitoneal administration of a therapeutic dose of 5-FU (30 mg/kg/mouse/day for 5 days). 3 days later, mice were sacrificed and the jejunum tissues were H&E stained for determination of the relative villus sizes (a) and immunohistochemically stained for measurement of the numbers of LGR5⁺-ISCs (b) and Ki67⁺-TA cells (c). Results are the mean \pm S.D. of 10 tissue sections/mouse (5 mice/group). Bars, 50 μ m. *, $p < 0.05$; **, $p < 0.01$.



Supplementary Figure 21 Cooperative induction of GFP^{high}-ISCs by Rspo1 and Slit2 in response to chemoradiotherapy. LGR5-GFP mice were given saline (-), rRspo1, rSlit2 or rRspo1 plus rSlit2 daily for 3 days. On day 2, they were treated with a single dose of 5-FU (300 mg/kg²¹; **a**) or WBI (10.4 Gy; **b**). The crypt specimens of their small intestines were harvested on day 6. Following staining with the anti-GFP Ab, they were quantified by flow cytometry. Results are the mean \pm S.D. of cytometric analysis for each group (five mice/group; 8 weeks old). *, $p < 0.05$; **, $p < 0.01$.